Available online at www.sciencedirect.com
SCIENCE DIRECT®
Thin Solid Films 497 (2006) 315 – 320
thin solid films
www.elsevier.com/locate/tsf

Surface plasmon assisted thermal coupling of multiple photon energies

A. Passian [a,*], A.L. Lereu [a,b], R.H. Ritchie [a], F. Meriaudeau [c], T. Thundat [a], T.L. Ferrell [a]

[a] *Department of Physics and Astronomy, University of Tennessee, Knoxville, TN 37996-1200, USA*
[b] *The Université de Bourgogne, Département de physique, 21011 Dijon, France*
[c] *The Université de Bourgogne, IUT du Creusot, Le2i, 71200 Le Creusot, France*

Received 21 July 2004; received in revised form 4 February 2005; accepted 1 September 2005
Available online 22 November 2005

Abstract

A novel optical effect can be observed in a thin gold foil due to the excitation of surface plasmons which permits a form of all-optical modulation at low pulse rates. Modulated excitation of surface plasmons by infrared photons is shown to couple to several beams at visible-photon energies. The coupling is manifested by the observation of the visible photons being pulsed by the action of the infrared pulses, and by the far field diffraction of the visible beams into concentric rings. When each visible beam also excites surface plasmons, then a quadratic dependence of the visible photon power upon the infrared incident power is measured. The decay of surface plasmons is implicated as the primary cause of thermally induced changes in the foil. The thermal effects dissipate in sufficiently small times so that operation up to the kilohertz range in pulse repetition frequency is obtained.

PACS: 73.20.Mf; 42.25.Bs; 42.79.Nv
Keywords: Surface plasmon coupling; Optical modulation; Thin metal films

1. Introduction

The quanta associated with the waves in bulk matter were first discussed in the early 1950s by Bohm and Pines [1], while the quanta associated with the surface waves were first described in 1957 by Ritchie [2]. The former are called "plasmons," and the latter are called "surface plasmons (SPs)," both initially being treated in terms of their contribution to energy losses by incident electron beams. The energy-loss spectrum of electrons penetrating metal foils displayed characteristic peaks which were shown to correspond to plasmon generation in the foil. The observation of multiple discrete energy losses was thus explained for bulk and surface media by invoking the plasmon concept within the context of second quantization. Photons cannot directly excite SPs for the important case of a plane-bounded medium, including the case of a thin foil. The simultaneous conservation of momentum and energy is not satisfied in this case. The circumvention of this condition can be attained by using metal particles, rough surfaces, gratings, or other symmetry-breaking material geometries allowing for consumption of the excess momentum of SPs. An important circumvention was proposed by Otto [3], and in a slightly different form, by Kretschmann [4]. Their concept is that the photon momentum can be increased to match that of the thin-film SP without altering the photon energy by simply using a transparent medium of optical index greater than unity as the incident medium. For a detailed historic account on the SPs, see Ref. [5].

SPs excited in a thin gold foil can decay by a number of mechanisms related to radiative, acoustic, and thermal coupling. When the exciting beam of wave vector k is set at the resonance angle θ, computed from the SP dispersion relation, the p-polarization component excites SPs of wave vector $\kappa = nk\sin\theta$, where n is the index of refraction of the substrate. The frequency range for which this occurs depends upon the optical properties of the material of the foil and upon the foil thickness, and is obtained from the dispersion relations of SPs and photons [6]. Although, the exponentially decaying field, and localized field enhancement associated with the excitation of SPs have had a great impact on application specific studies, such as near field phenomena [7], nanotechnologies [8], and biosensing [9], little attention has been devoted to thermo-

* Corresponding author. Tel.: +1 865 574 6219; fax: +1 865 574 6210.
E-mail address: passianan@ornl.gov (A. Passian).

0040-6090/$ - see front matter © 2005 Elsevier B.V. All rights reserved.
doi:10.1016/j.tsf.2005.09.016

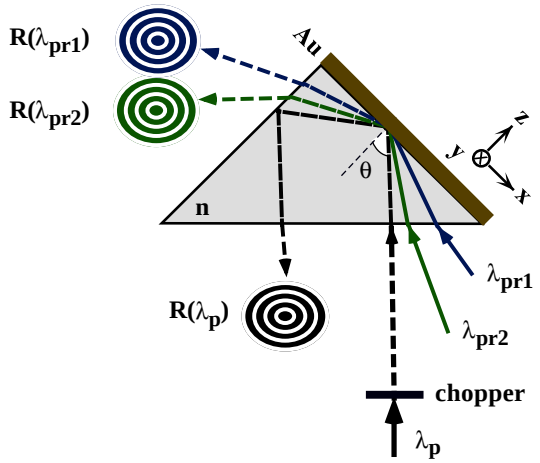

Fig. 1. Schematics of the experimental arrangement for SPAC. The gold film is defined by the *xy*-plane. The incident infrared beam is labeled λ_p, while all the incident visible beams are labeled λ_{pri}; with $i=1, 2, \ldots$, and the corresponding reflected beams are labeled by R.

optical and related processes involving SPs. The aim of this paper is to present first experimental results of thermo-optical studies utilizing SPs, which has not been previously reported. Our attempt to introduce the SP as an essential component in such processes, may therefore open new possibilities in fields such as photothermal effect [10–15].

If the information in an incoming beam of energy $E_i=\hbar\omega_i$, and intensity I_i is transfered, by an interaction, to an outgoing beam of energy $E_o=\hbar\omega_o$, and intensity I_o, then one may infer that an energy scaling $\omega_o=\alpha(\lambda_i,\lambda_o)\omega_i$, and a similar intensity scaling of the information have occured, where α is the wave length (λ)-dependent scaling factor. In the present study, the Kretschmann configuration is shown to permit such a coupling scheme involving several photon energies (Fig. 1). The observed coupling results in simultaneous energy and intensity scaling, which are here reported for the case of a $\lambda=1.55$ μm communication laser, and several beams in the visible spectrum. In order to study the rate of information transfer, we here use the intensity modulation $I_o=\Gamma(f)I_i$, that is, we modulate the incoming (pump) beam in a frequency f range below 10 kHz, where $\Gamma(f)$ represents the modulation function, which in this work is simply that of a mechanical chopper. Several unpulsed beams from lasers of visible wavelengths are shown to be pulsed by the action of $\Gamma(f)$; a process henceforth referred to as SP assisted coupling (SPAC). In the present situation, the SPs act as an intermediate and essential excitation. Moreover, thermal effects dissipate relatively quickly in a gold foil due to the geometry and the high thermal conductivity, allowing kilohertz pulse rates.

Direct photo-thermal effects are clearly distinct from the case presented here. In the photo-thermal effect, direct heating is utilized to induce, for example, a phase change as in the local melting of a material. The photo-thermal effect is created in some instances by focusing a light beam in order to produce a high thermal gradient and the associated local phase effects that can provide the equivalent of a very small lens or diffractive element.

2. Experimental procedure

A diagram of the core apparatus and optical paths is shown in Fig. 1. This is the Kretschmann configuration with additional laser beams incident on the gold foil within the exact same foil area. The 29.5-nm-thick gold film (*xy*-plane), vacuum evaporated on the side of a right-angled triangular quartz prism (index of refraction $n=1.46$), supports plasmon excitation with optimized absorption for the wavelength $\lambda_p=1550$ nm. The infrared "pump" laser (λ_p) is pulsed with a mechanical chopper at lower frequencies, and through the use of an acousto-optic modulator for higher frequencies. A lock-in amplifier is then used to extract the modulated reflected (R) beams detected by photomultiplier tubes (PMTs) located at the optical axis of the beams. A laser beam profiler and an infrared viewing camera were used for beam diagnostics and recording. The low power visible "probe" laser beams (He–Cd's $\lambda_{pr1}=442$ nm, Ar^+'s $\lambda_{pr2}=515$ nm, and a He–Ne at $\lambda_{pr3}=632.8$ nm used here with typical power levels in the range 1–20 mW) are not pulsed and are initially and independently set so that minimal reflection occurs. Thus, using wave plates, all beams are p-polarized and directed to be incident on the gold foil at the respective resonance angle, i.e., at the peak angle for which the minimum of reflectivity occurs ($\theta_p=43.6°$, $\theta_{pr1}=60°$, $\theta_{pr2}=53°$, $\theta_{pr3}=46.9°$) as predicted by the simulation displayed in

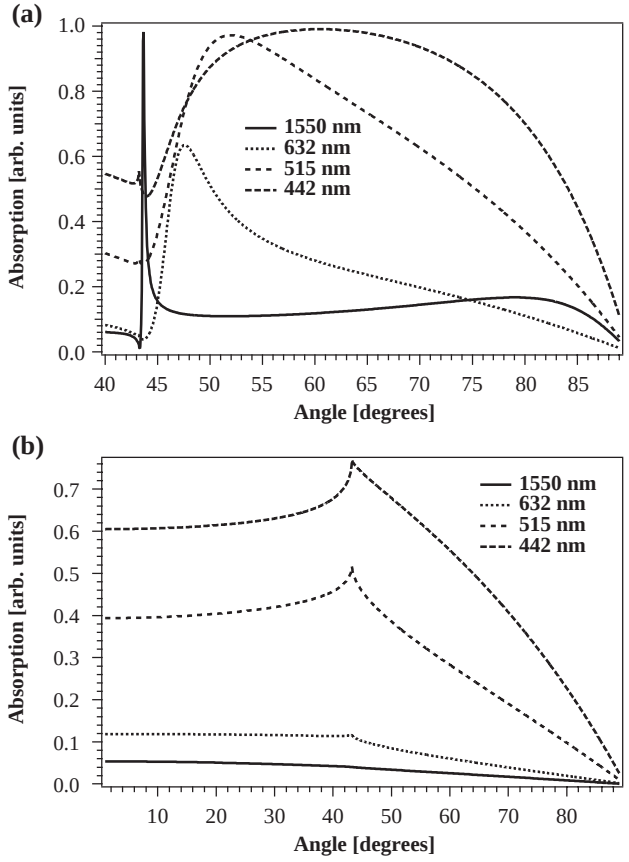

Fig. 2. The simulated absorption of a 29.5-nm gold foil on a quartz substrate at the photon energies considered in this work. The film thickness was optimized for the infrared line. (a) displays the p-polarization spectra, while (b) shows the corresponding s-polarization.

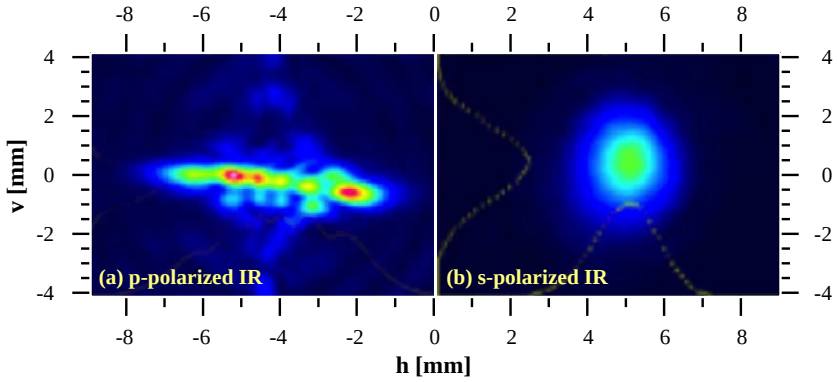

Fig. 3. The influence of the polarization state of the IR pump beam on the reflected probe beam profile. In (a), the diffracted reflected probe beam $R(\lambda_{pr1})$ is recorded under the influence of the IR SP, while in (b) no effect can be observed due to s-polarization state of the IR beam.

Fig. 2a. The wave plates are also used to rotate the polarization of all beams in order to examine the polarization dependence of the coupling. We note here that while the incoming pump beam is p-polarized, in order that maximum resonance absorption (due to excitation of surface plasmons) occurs, the probe beams can be p- or s-polarized. Fig. 2 compares the absorption at photon wavelengths used for p- and s-polarizations. As can be seen from Fig. 2b, there is a substantial absorption ($\approx$56% at 60° for λ_{pr1}) for s-polarization.

3. Results and discussions

Simultaneous excitation of the SPs at several visible photon energies (λ_{pri}, $i=1, 2, \ldots$) is modulated by the SP excitation due to the higher power infrared photons (λ_p). This modulation can be detected in all the reflected beams $R(\lambda_{pri})$, $i=1, 2, \ldots$ for both p- and s-polarizations. When the infrared beam is on at the same time as the visible beams, the SP excitation conditions are modified so that there are measurable reflected photons in

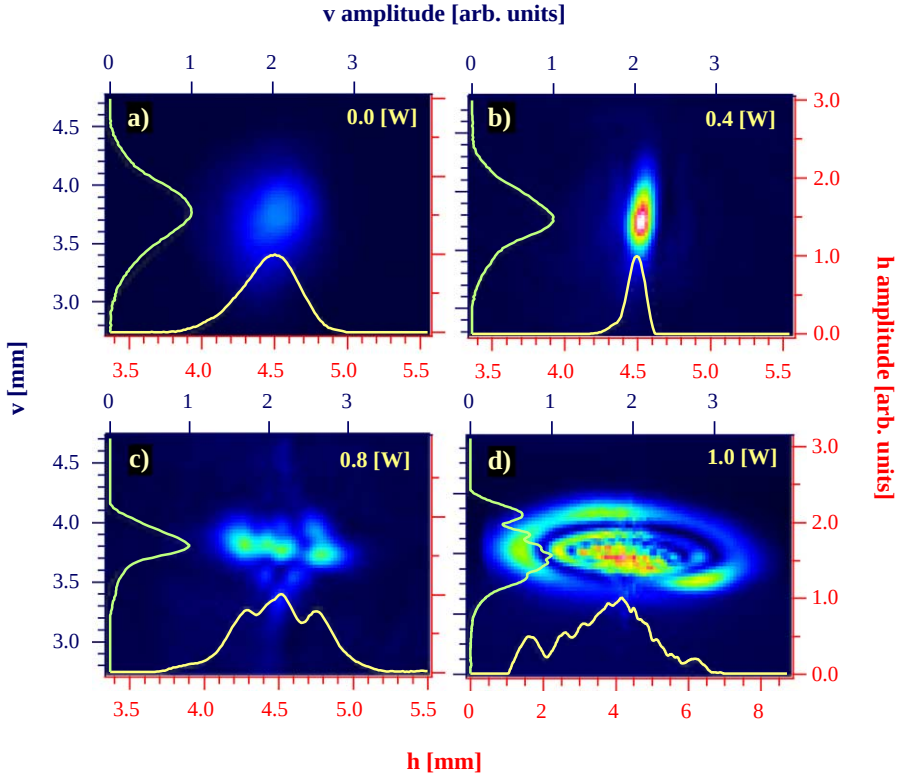

Fig. 4. The SP-assisted spatial modulation of the reflected probe beam $R(\lambda_{pr1}=442$ nm). (a) A 20-mW beam loses energy to the SPs in a 29.5-nm-thick gold foil to generate a 0.3-mW reflected beam, which is recorded a few centimeters ($\approx$8 cm) away from the exit face of the prism in the *hv*-plane, a plane perpendicular to the direction of $R(\lambda_{pr1})$. The resonance conditions are subsequently modified by the excitation of SPs due to the infrared beam λ_p as evident from the sequence of profiles displayed in (b) and (c) recorded, in the *hv*-plane, as a function of increasing power levels of λ_p beam as inscribed. The vertical and horizontal line profiles displayed are taken through the point of maximum intensity in the images. In (d), the measurement is repeated at a further distance ($\approx$20 cm) from the exit face of the prism. During this process, a 44% relative increase of the $R(\lambda_{pr1})$ beam power is measured, while the horizontal FWHM decreases initially from 0.5 mm (a) to 150 μm (b), whereafter it increases to about 1 mm (c).

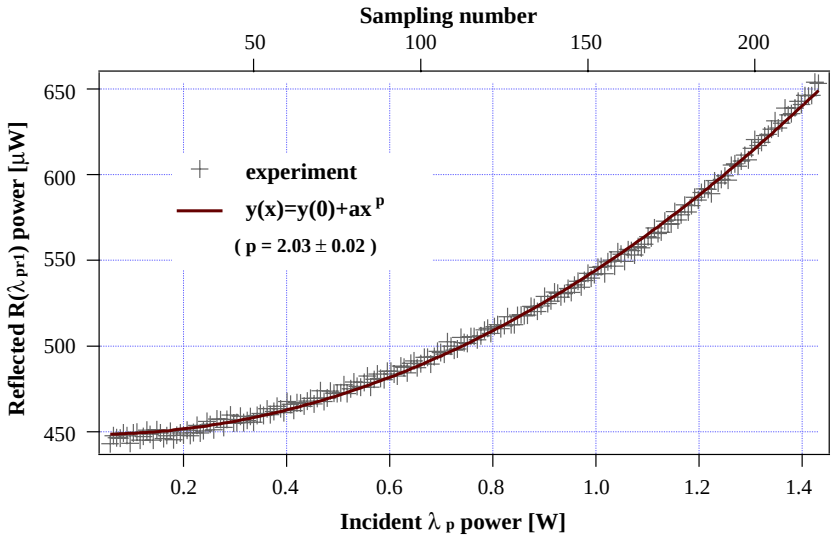

Fig. 5. The measured variation of SPAC magnitude. Reflected visible power as a function of incident infrared excitation λ_p power. A 20-mW p-polarized λ_{pr1} beam incident at 60° undergoes resonant absorption in the film to generate the reflected power $R(\lambda_{pr1})$. As can be seen from the inset, a quadratic fit describes the magnitude of the SPAC fairly well.

the visible. If the infrared beam is off (infrared SPAC disabled) then the reflected visible light is minimal.

The reflected beams are observed to be pulsed, and are measured by the lock-in amplifier which differentiate the pulsed beams from any unpulsed light. The amplitudes of modulation of the probe beams drop continuously to zero for the same modulation frequency if the polarization state of the pump infrared beam is varied continuously from p→s. Qualitatively, this can be explained in Fig. 2, where an approximately 99% absorption at the peak resonance angle for p-polarization (Fig. 2a) is reduced to a mere 3% in the case of s-polarization (Fig. 2b). This is also illustrated in Fig. 3, displaying the reflected p-polarized λ_{pr1} beam, when the pump infrared beam polarization is rotated from p- (Fig. 3a) to s- (Fig. 3b) polarization. Fig. 3a shows an expansion of the reflected λ_{pr1} beam which, collapses to its original form when the IR beam is s-polarized, as can be seen in Fig. 3b. However, the polarization states of the incident visible beams only influence the power levels of the reflected modulated beams (higher for s-polarization and lower for p).

The pulsing action during each cycle of modulation takes on the form of a physical redistribution of the power density of the reflected probe beams similar to a lateral convergence for moderate infrared power levels, and a divergence for higher power levels. This is shown in Fig. 4 for λ_{pr1}, where such a redistribution is demonstrated in a sequence of spatial beam profiles recorded at increasing infrared power levels. As can be seen, an initial squeezing of the unmodulated reflected λ_{pr1} beam evolves into a laterally distributed beam. Simultaneously, an increase in the power level of the reflected visible beams is also measured that depends (quadratically) on the infrared λ_p power level for moderate ranges as shown in Fig. 5. The latter, measuring the strength of the SPAC, can be attributed to a perturbation of the resonance conditions of the SPs excited by the visible beams due to the infrared excitation. A measurement of the frequency dependence of such a coupling is presented in

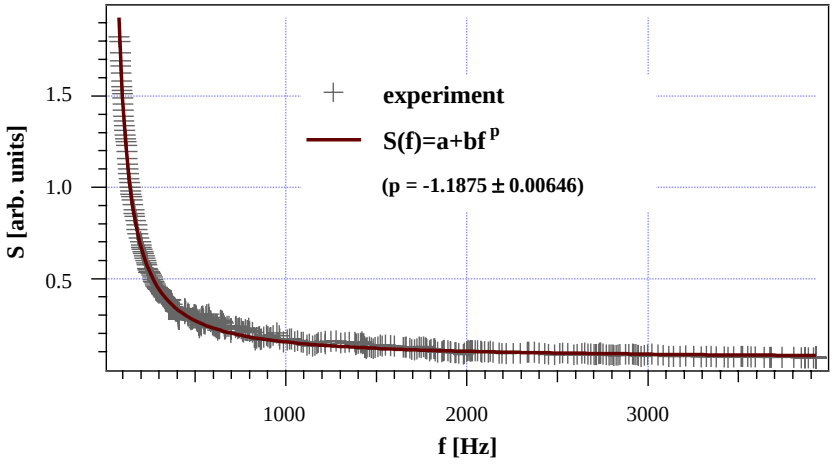

Fig. 6. The measured frequency dependence of SPAC. The modulation of the reflected visible $R(\lambda_{pr1})$ power as a function of the modulated infrared excitation λ_p power (symbols). The solid curve represents a numeric fit to an inverse function which appears to describe the frequency dependence of SPAC well.

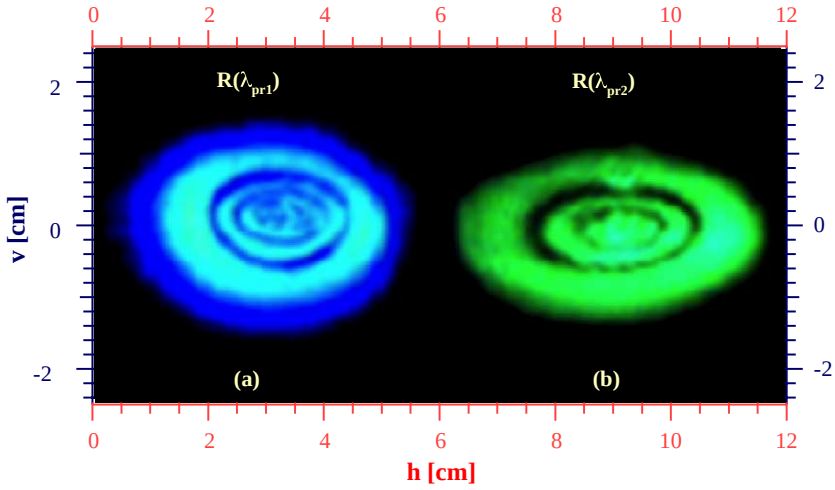

Fig. 7. Beam characteristics were studied for the modulated reflected beams by recording the profile in the *hv*-plane, of the projected beams at various distances from the foil. At further distances (≈2 m), the beams diffract into several clearly discernible concentric rings as shown in the images in (a) and (b) for the two simultaneously recorded reflected beams λ_{pr1} and λ_{pr2}. The more intense the infrared SP excitation, the higher the number of rings and the larger the radius. The measurements shown are for λ_p incident power of 1 W at the peak resonance angle.

Fig. 6, which displays a nearly inverse behavior with modulation frequency *f*. As depicted in Fig. 1, reflected visible beams appear, when observed at long distances from the gold film, to be diffracted as in the pattern of a circular aperture leading to a circular interference pattern as shown in the two profiles in Fig. 7 and in Fig. 4d. When the IR SP excitation is suddenly discontinued, the observed ring system will collapse into a single spot, with a diameter of the order of the incident probe beam, at which point if the IR is suddenly reinstalled the single spot will resume the original ring system.

Also noteworthy is that, although much weaker (for the used visible/infrared power level ratio, which can also be >1), we observed the reverse process, i.e., the SPAC mediated effect of the visible λ_{pr1} beam on the infrared λ_p reflected beam to be measurable. The reflected λ_p beam undergoes a similar deformation as a result of turning any of the visible λ_{pri}, $i=1, 2, \ldots$ beams on. This interplay is minimal when the polarization state of the λ_{pr1} beam is shifted from p→s, and absent when also λ_p is s-polarized. As an example, for an incident IR power of 165 mW, turning a 20-mW λ_{pr1} beam on, under otherwise similar experimental conditions, results in a roughly 2% (vertical and horizontal) beam profile distortions. Variation of any of the parameters of the infrared beam, such as angle of incidence, polarization state, intensity, and frequency constitutes a modulation channel for all the visible beams. A distinct advantage of this system is the basic simplicity.

We believe that the observed effects can be explained on the basis of the energy deposited into the gold foil by the decaying SPs. This energy deposition thermally modifies the local optical properties of the foil. This requires modeling of the temperature dependence of the complex dielectric function of the gold foil (in conjunction with the induced macroscopic variations such as volume expansion of the involved multilayer). For example, a Gaussian modulated volume expansion of the excitation region may result in a variation in the local electron density, which in turn shifts the local value of the dielectric function, and thus alters the SP dispersion relation. We estimate that if heat is suddenly liberated in a medium with thermal diffusivity *K*, then the time characterizing the decay of the temperature distribution, over for example a propagation distance of $\lambda/2$, toward a constant value is $\lambda^2/4K$. In a gold foil with $K=1.17$ cm^2 s^{-1} and for $\lambda=\lambda_p=1550$ nm, the characteristic time is ≈5 ns. We therefore surmise that the interference in the various parts of this region gives rise to the formation of the observed rings.

4. Conclusions

A novel thermo-optic effect in the Kretschmann configuration has been observed that is analogous to thermal lensing in that a temperature gradient is necessary for the observation of the effect. However, in contrast to thermal lensing, the excitation of surface plasmons is necessary, and as such any parameters that may alter the conditions for the coherent collective oscillations of the conduction electrons will alter the effect. Modulation of visible light by an infrared communication laser has been demonstrated within the audio range of frequencies. Audio signals carried by infrared can therefore be converted into a range of colors. Similarly, red, green, and blue laser wavelengths can be modulated by infrared signals that carry visual display information since visual persistence allows use of low-frequency modulation. Other color combinations can be used as necessary to create a full-color display from separately modulated infrared signals. Other applications may include additions to biosensing instruments that rely upon the Kretschmann configuration, and the transfer of infrared signals to human-perceived “white light” obtained by mixing of primary colors. The large thermal conductivity of gold has been presented as allowing to pass information from the infrared to the visible at low frequencies.

A number of parameters remain to be determined, including the temperature dependence of the effects. A much more thorough investigation is warranted in order to delineate applications and limitations. However, the basic effects can

be expressed in a straightforward manner in a relatively simple experiment. Use of an appropriate substrate for the gold foil in the Kretschmann configuration would permit the observed effects at lower infrared power levels. Such a substrate would need to be altered by the exponentially decaying SP field near the foil in a volume-dependent manner. Alterations that would enhance the effects include changes in either the real or imaginary part of the optical index or rotation of the polarization state.

Acknowledgements

This work was supported in part by a contract with R&D Limited Liability Partnerships, Inc., and the suggestion of potential applications to the optical communications field involving the standing SP concepts are gratefully acknowledged [16]. This work was also supported by the Defense Advanced Research Projects Agency under BAA 99-32 for development of a controllable diffraction element for spectroscopy using standing SPs.

References

[1] D. Bohm, D. Pines, Phys. Rev. 82 (1951) 625.
[2] R.H. Ritchie, Phys. Rev. 106 (1957) 847.
[3] A. Otto, Z. Phys. 216 (1968) 398.
[4] E. Kretschmann, Z. Phys. 241 (1971) 313.
[5] T.L. Ferrell, T.A. Callcott, R.J. Warmack, Am. Sci. 73 (1985) 344.
[6] H. Raether, Surface Plasmons on Smooth and Rough Surfaces and on Gratings, Sringer, Berlin, 1988.
[7] S. Kawata, Near Field Optics and Surface Plasmon Polaritons, Sringer, Berlin, 2001.
[8] J. Tominaga, D.P. Tsai, Optical Nanotechnologies: The Manipulation of Surface and Local Plasmons, Sringer, Berlin, 2003.
[9] J. Homola, S.S. Yee, G. Gauglitz, Sens. Actuators, B 54 (1999) 315.
[10] T. Inagaki, J.P. Goudonnet, E.T. Arakawa, Opt. Sci. 58 (1988) 156.
[11] K.D. Cole, Int. J. Thermophys. 25 (2004) 1567.
[12] E. Welsch, K. Ettrich, D. Ristau, U. Willamowski, Int. J. Thermophys. 20 (1999) 965.
[13] J.A. Batista, D. Takeuti, A.M. Mansanares, E.C. da Silva, Anal. Sci. 17 (2001) s73.
[14] B.C. Li, S.Y. Zhang, Int. J. Thermophys. 19 (1998) 615.
[15] S. Wu, N.J. Dovichi, J. Appl. Phys. 67 (1990) 1170.
[16] D.G. Bottrell, T.M. Capser, U.S. Patent No. 6,587,252, 1 July (2003).